# Torsional Effects on the One-Bond $^{13}C$–$^{13}C$ Spin Coupling Constant in Ethylene Glycol: Insights into the Behavior of $^1J_{CC}$ in Carbohydrates†

**Ian Carmichael,*,‡ Daniel M. Chipman,‡ Carol A. Podlasek,§ and Anthony S. Serianni*,§**

*Contribution from the Radiation Laboratory and Department of Chemistry and Biochemistry, University of Notre Dame, Notre Dame, Indiana 46556*

*Received March 11, 1993®*

**Abstract:** Recent NMR studies of a series of $^{13}C$-enriched carbohydrates and their derivatives have revealed that $^1J_{CC}$ in OH–C–C–OH fragments is affected by the C–C dihedral angle. This and other related correlations are explored in detail in this study by measuring and computing $^1J_{CC}$ values in simple model compounds. The *ab initio* computational methods used are validated through a comparison of absolute values and trends observed for a variety of calculated and experimental $^1J_{CC}$. Good agreement with experiment is found when electron correlation is thoroughly treated at the sophisticated QCISD(T) level. Although $^1J_{CC}$ values computed at the SCF level are much larger than those observed experimentally, the electron correlation corrections remain relatively independent of conformation, so that SCF calculations are very useful for examining trends. Results for ethane, ethanol, ethylene glycol, and glycolaldehyde hydrate indicate that $^1J_{CC}$ increases with the number of hydroxyl substituents on the CC fragment. Calculations of the dependence of $^1J_{CC}$ on C–C torsion in ethylene glycol agree with experimental data for carbohydrates, indicating that the coupling is largest when the hydroxyl substituents are *trans* and smaller for *gauche* geometries. A significant new finding in this study is that $^1J_{CC}$ in ethylene glycol fragments depends to an even larger extent on the C–O torsions, reaching a maximum when the hydroxyl proton is anti to a carbon and a minimum in *gauche* configurations. Thus, in addition to the relative C–C torsion, it is also important to consider the conformational behavior of the C–O bonds. This observation imposes limitations on the use of $^1J_{CC}$ as a structural probe, as in some cases information about C–C *and* C–O torsions will not be available. In situations where one of these variables is known (more likely the C–C torsion), $^1J_{CC}$ may be useful to probe the remaining variable (e.g., hydroxyl proton orientation in solution). The behavior of $^1J_{CC}$ in $(OH)_2$–C–C–OH fragments such as those found in aldofuranosyl and aldopyranosyl rings was also examined, using the trihydroxyl compound glycolaldehyde hydrate and D-mannopyranose as model systems. Results indicate that the correlations found between $^1J_{CC}$ and C–C and C–O torsions in ethylene glycol are also maintained in these systems.

## Introduction

Since first reported by Karplus[1] in 1959, vicinal spin–spin coupling constants ($^3J$) derived from NMR spectra have been used extensively to elucidate molecular structure due to their dependence on molecular dihedral angles, $\theta$. These couplings may be homonuclear (e.g., $^3J_{HH}$ and $^3J_{CC}$) or heteronuclear (e.g., $^3J_{CH}$ and $^3J_{CP}$) and apparently respond to $\theta$ in a similar fashion (i.e., bell-shaped curves with maxima at $\theta = \sim 0$ and $\sim 180°$ and a minimum at $\theta = \sim 90°$). For example, Karplus relationships have been proposed for $^3J_{HH}$ coupling pathways, including HCCH,[2,3] HCNH,[4,5] and HCOH,[6] and $^3J_{CH}$ coupling pathways, including CCCH,[7] COCH,[8,9] and CCNH.[10] In addition to $^3J$, homonuclear and heteronuclear $^2J$ values also depend on molecular structure. For example, $^2J_{HCH}$ is affected by the HCH bond angle, with increasing angles leading to an algebraic increase in this coupling.[11] For carbohydrates, vector[7,12,13] and projection sum[14] rules have been developed that relate $^2J_{CCH}$ to substituent geometry on a CCH fragment, whereas $^2J_{CCC}$ values are notably affected by the orientation of terminal hydroxyl substituents on the CCC fragment.[15,16] Applications of $J_{CH}$ and $J_{CC}$ to problems in organic stereochemistry and conformational analysis have been reviewed by Marshall.[17]

Despite their application in structure determination in a wide range of molecules, the utility of longer-range spin couplings is sometimes compromised in larger compounds in which NMR line broadening can be substantial, thereby complicating or preventing their measurement. This limitation has led to a renewed interest in the dependence of the considerably larger one-bond spin couplings (e.g., $^1J_{CH}$ and $^1J_{CC}$) on molecular structure and conformation. $^1J_{CH}$ and $^1J_{CC}$ depend on the percent s-character of the carbons in CH[18] and CC[19] bonds, respectively.

* Authors for correspondence.

† This is Document No. NDRL-3576 from the Notre Dame Radiation Laboratory.

‡ Radiation Laboratory.

§ Department of Chemistry and Biochemistry.

® Abstract published in *Advance ACS Abstracts*, October 1, 1993.

(1) Karplus, M. *J. Chem. Phys.* **1959**, *30*, 11–5.
(2) Haasnoot, C. A. G.; de Leeuw, F. A. A. M.; Altona, C. *Tetrahedron* **1980**, *36*, 2783–92.
(3) Haasnoot, C. A. G.; de Leeuw, F. A. A. M.; de Leeuw, H. P. M.; Altona, C. *Org. Magn. Reson.* **1981**, *15*, 43.
(4) Bystrov, V. F. *Prog. Nucl. Magn. Reson. Spectrosc.* **1976**, *10*, 41–82.
(5) Pardi, A.; Billeter, M.; Wüthrich, K. *J. Mol. Biol.* **1984**, *180*, 741–51.
(6) Fraser, R. R.; Kaufman, M.; Morand, P.; Govil, G. *Can. J. Chem.* **1969**, *47*, 403–9.
(7) Schwarcz, J. A.; Perlin, A. S. *Can. J. Chem.* **1972**, *50*, 3667.
(8) Perlin, A. S.; Hamer, G. K. In *Carbon-13 NMR in Polymer Science*; Pasika, W. M., Ed.; ACS Symposium Series 103; American Chemical Society: Washington, DC, 1979; p 123.
(9) Tvaroska, I.; Hricovini, M.; Petrakova, E. *Carbohydr. Res.* **1989**, *189*, 359–62.
(10) Bystrov, V. F.; Gavrilov, Y. D.; Ivanov, V. T.; Ovchinnikov, Y. A. *Eur. J. Biochem.* **1977**, *78*, 63.
(11) Maciel, G. E.; McIver, J. W.; Oslund, N. S.; Pople, J. A. *J. Am. Chem. Soc.* **1970**, *92*, 4151–7.
(12) Schwarcz, J. A.; Cyr, N.; Perlin, A. S. *Can. J. Chem.* **1975**, *53*, 1872.
(13) Cyr, N.; Hamer, G. K.; Perlin, A. S. *Can. J. Chem.* **1978**, *56*, 297.
(14) Bock, K.; Pedersen, C. *Acta Chem. Scand.* **1977**, *B31*, 354.
(15) King-Morris, M. J.; Serianni, A. S. *J. Am. Chem. Soc.* **1987**, *109*, 3501.
(16) Wu, J.; Bondo, P. B.; Vuorinen, T.; Serianni, A. S. *J. Am. Chem. Soc.* **1992**, *114*, 3499.
(17) Marshall, J. L. *Carbon-Carbon and Carbon-Proton NMR Couplings: Applications to Organic Stereochemistry and Conformational Analysis*; Verlag Chemie International: Deerfield Beach, FL, 1983.
(18) Müller, N.; Pritchard, D. E. *J. Chem. Phys.* **1959**, *31*, 768.

0002-7863/93/1515-10863$04.00/0 

In aldopyranosyl rings, $^1J_{C_1H_1}$ is affected by CH bond orientation, with equatorial CH bonds having larger couplings (~170 Hz) than axial CH bonds (~160 Hz).[14,20,21] This difference provides a means to assign anomeric configuration in aldopyranoses and their glycosides. Recently, $^1J_{CH}$ was used to assess glycoside linkage conformation in oligosaccharides[22] and preferred furanose ring conformation in RNA oligomers.[23]

Recent studies of $^1J_{CC}$ in a series of carbohydrates and their derivatives have revealed a consistent pattern of potential value for structure elucidation. $^1J_{C1,C2}$ in aldofuranose rings[24-26] is consistently larger when O1 and O2 are *trans* (**1**) than when these substituents are *cis* (**2**). $^1J_{C1,C2}$ in aldopyranoses[15] and 2-ketofuranosyl[27] rings behave similarly; for example, $^1J_{C1,C2}$ values are larger in α-D-mannopyranose (**3**) and α-D-talopyranose (**4**) than in β-D-mannopyranose (**5**) and β-D-talopyranose (**6**), and $^1J_{C2,C3}$ is larger in methyl α-D-fructofuranoside (**7**) than in methyl β-D-fructofuranoside (**8**). These data suggest that $^1J_{CC}$ in HO–C–C–OH fragments is affected by the C–C dihedral angle, with larger couplings associated with conformations having both oxygen atoms *trans* or nearly *trans*. This correlation has been explored in this study by computing $^1J_{CC}$ values for various conformations of the simple model compound, ethylene glycol ($HOCH_2CH_2OH$) (**9**), in which both C–C and C–O bond torsions were systematically varied. *Ab initio* methods used to calculate $^1J_{CC}$ values for **9** were validated through a comparison of absolute values and trends observed in computed and experimental $^1J_{CC}$ for C–C fragments appended with different numbers of hydroxyl groups.

Several calculations of $^1J_{CC}$ are also reported for ethanol (**10**), with one hydroxyl substituent, and glycolaldehyde hydrate (**11**), $HOCH_2$–$CH(OH)_2$. Trends in $^1J_{CC}$ are explored in calculations at the self-consistent field (SCF) level, while the important effects of electron correlation are investigated at several strategically located points on the generated torsional hypersurfaces.

One-bond carbon–carbon coupling constants calculated at the SCF level are much greater in magnitude than those observed experimentally, and second-order Møller–Plesset perturbation theory (MP2) treatments consistently exaggerate the required corrections. A much more thorough treatment of electron correlation is employed here. The effect of amplitudes due to double replacements in the Hartree–Fock (HF) self-consistent field wave function is calculated to all orders by the coupled-cluster doubles (CCD) procedure.[28,29] Further, the effect of configurations reached by single replacements in the SCF reference state is also incorporated in a size-consistent fashion. Lastly, triple excitations are included perturbatively to give the QCISD(T) model, recently proposed by Pople *et al.*[30] and shown to give an accurate account of electron correlation effects in a wide variety of circumstances. The magnetic coupling constants are then obtained by finite-field (double) perturbation theory[31] by performing calculations at this high level of theory in the presence of hypothetical nuclear moments placed on the coupled nuclei. It should be noted that only the Fermi contact component of the coupling constant is recovered in this procedure. However, it is precisely this mechanism which generally dominates the spin–spin coupling between carbon nuclei, thus validating this computational approach.[17]

Due to the presence of the magnetic perturbations, calculations at the SCF level necessarily employ the unrestricted Hartree–Fock (UHF) approach. The correlated calculations described above are then based on the UHF wave function as a single reference determinant and should be more properly denoted as UMP2 etc. Explicit designation of the underlying spin-unrestricted wave function has been omitted below to simplify the notation.

The QCISD(T) model of electron correlation has proven particularly successful in predicting the Fermi contact hyperfine splitting in a large variety of open-shell radical species[32-34] and has been found[35] to produce similarly satisfactory results for the indirect spin–spin couplings in closed-shell molecules such as those under investigation here.

## Experimental Section

**Compounds.** D-Mannose was purchased from Sigma Chemical Co.; a sample was dissolved in $H_2O$, concentrated to a syrup at 30 °C in vacuo, and crystallized from ethanol (the α-pyranose crystallizes preferentially under these conditions). [1-$^{13}$C]Ethanol (99 atom % $^{13}$C), $^2H_2O$ (98 atom % $^2$H), and K$^{13}$CN (99 atom % $^{13}$C) were purchased from Cambridge Isotope Laboratories.

D-[1-$^{13}$C]Mannose (99 atom % $^{13}$C) was prepared from K$^{13}$CN and D-arabinose by cyanohydrin reduction,[36,37] and D-[2-$^{13}$C]mannose (99 atom % $^{13}$C) was prepared from D-[1-$^{13}$C]glucose by molybdate-catalyzed epimerization.[38] Both $^{13}$C-labeled D-mannoses were crystallized from ethanol to give solid samples of the α-pyranose.

DL-[1-$^{13}$C]-1,2-Dihydroxypropane (99 atom % $^{13}$C) was prepared by reduction of DL-[1-$^{13}$C]-1,2-dihydroxypropanal (DL-[1-$^{13}$C]lactaldehyde) with $NaBH_4$. DL-[1-$^{13}$C]-1,2-Dihydroxypropanal was prepared from K$^{13}$CN and acetaldehyde by cyanohydrin reduction.[39] $^{13}$C Chemical shifts of DL-[1-$^{13}$C]-1,2-dihydroxypropane: 68.0 ppm, C1; 69.4 ppm, C2; 19.4 ppm, C3 ($^1J_{C1,C2}$ = 41.3 Hz; $^2J_{C1,C3}$ = 2.3 Hz).

[1-$^{13}$C]Glycolaldehyde (99 atom % $^{13}$C) was prepared from K$^{13}$CN and formaldehyde as described previously.[39]

**NMR Spectroscopy.** $^1$H (500 MHz) and $^1$H-decoupled $^{13}$C (125 MHz) NMR spectra were obtained on a Varian VXR-500S (UNITY) 500-MHz FT-NMR spectrometer located in the Lizzadro Magnetic Resonance Research Center at the University of Notre Dame. Hydroxyl proton signals were observed in D-mannose (natural and $^{13}$C-labeled) by dissolving crystalline samples in dry DMSO-$d_6$ (Aldrich; predried over 3-Å molecular sieves) to give solutions 5 mM in sugar; NMR spectra were collected at 30 °C. $^{13}$C–$^{13}$C spin coupling constants were measured in $^2H_2O$ solvent (~0.5 M in labeled compound) at 30 °C. Reported $J_{CC}$ and $J_{HH}$ values are accurate to ±0.1 Hz.

**Computational Details.** All calculations reported here were performed with a modified version of the GAUSSIAN 90 series of programs[40] running on Convex C120 and C240 minisupercomputers.

Exploratory calculations employed small valence double-ζ and full double-ζ basis sets, which may be denoted 6-31G and [4s2p|2s], respectively. In the latter basis set descriptor, the vertical rule separates the set of contracted Gaussian functions on the heavy atoms, here carbon and oxygen, from those on hydrogen. The effects of inclusion of polarization (d-) functions on the heavy atoms, denoted 6-31G* and [4s2p1d|2s], respectively, and p-functions on the hydrogens, [4s2p1d|2s1p],

(19) Schulman, J. M.; Newton, M. D. *J. Am. Chem. Soc.* **1974**, *96*, 6295–7.
(20) Bock, K.; Pedersen, C. *J. Chem. Soc., Perkin Trans. 2* **1974**, 293.
(21) Bock, K.; Pedersen, C. *Acta Chem. Scand.* **1975**, *B29*, 258.
(22) Tvaroska, I. *Carbohydr. Res.* **1990**, *206*, 55–64.
(23) Varani, G.; Tinoco, I., Jr. *J. Am. Chem. Soc.* **1991**, *113*, 9349.
(24) Serianni, A. S.; Barker, R. *J. Org. Chem.* **1984**, *49*, 3292.
(25) Snyder, J. R.; Serianni, A. S. *Carbohydr. Res.* **1987**, *163*, 169.
(26) Wu, J.; Serianni, A. S. *Carbohydr. Res.* **1991**, *210*, 51.
(27) Vuorinen, T.; Serianni, A. S. *Carbohydr. Res.* **1990**, *209*, 13.
(28) Pople, J. A.; Krishnan, R.; Schlegel, H. B.; Binkley, J. S. *Int. J. Quantum Chem.* **1978**, *14*, 545–60.
(29) Bartlett, R. J.; Purvis, G. D. *Int. J. Quantum Chem.* **1978**, *14*, 561–81.
(30) Pople, J. A.; Head-Gordon, M.; Raghavachari, K. *J. Chem. Phys.* **1987**, *87*, 5968–75.
(31) Kowalewski, J.; Laaksonen, A.; Roos, B.; Siegbahn, P. *J. Chem. Phys.* **1979**, *71*, 2896–902.
(32) Carmichael, I. *J. Chem. Phys.* **1990**, *93*, 863–4.
(33) Carmichael, I. *J. Phys. Chem.* **1991**, *95*, 108–11.
(34) Carmichael, I. *J. Phys. Chem.* **1991**, *95*, 6198–201.
(35) Carmichael, I. *J. Phys. Chem.* **1993**, *97*, 1789–92.
(36) Serianni, A. S.; Nunez, H. A.; Barker, R. *Carbohydr. Res.* **1979**, *72*, 71.
(37) Serianni, A. S.; Vuorinen, T.; Bondo, P. B. *J. Carbohydr. Chem.* **1990**, *9*, 513.
(38) Hayes, M. L.; Pennings, N. J.; Serianni, A. S.; Barker, R. *J. Am. Chem. Soc.* **1982**, *104*, 6764.
(39) Serianni, A. S.; Clark, E. L.; Barker, R. *Carbohydr. Res.* **1979**, *72*, 79.
(40) Frisch, M. J.; Head-Gordon, M.; Trucks, G. W.; Foresman, J. B.; Schlegel, H. B.; Raghavachari, K.; Robb, M. A.; Binkley, J. S.; Gonzales, C.; DeFrees, D. J.; Fox, D. J.; Whiteside, R. A.; Seeger, R.; Melius, C. F.; Baker, J.; Martin, R. L.; Kahn, L. R.; Stewart, J. J. P.; Topiol, S.; Pople, J. A. *GAUSSIAN 90*, Revision G; Gaussian, Inc.: Pittsburgh, PA, 1990.

**Table I.** Fermi Contact Contribution to the Carbon–Carbon Nuclear Spin–Spin Coupling Constant, $^1J_{CC}$, in Ethanol[a]

| basis | method | | | | |
|---|---|---|---|---|---|
| | SCF | MP2 | CCD | QCISD | QCISD(T) |
| 6-31G | 73.1 | 47.0 | 48.2 | 53.6 | 53.1 |
| 6-31G* | 61.7 | 36.2 | 38.6 | 43.3 | 42.3 |
| [4s2p\|2s] | 79.3 | 43.2 | 44.7 | 52.0 | 51.5 |
| [4s2p1d\|2s] | 74.6 | 34.5 | 38.4 | 45.9 | 44.8 |
| [4s2p1d\|2s1p] | 73.6 | 34.1 | 38.7 | 46.0 | 44.7 |
| [5s2p\|2s] | 71.9 | 39.0 | 40.5 | 46.6 | 46.1 |
| [5s2p1d\|2s] | 68.8 | 31.0 | 34.8 | 41.8 | 40.6 |

[a] Values in hertz from calculations performed at the experimental geometry of the *trans* conformer.[41] The experimental value of $^1J_{CC}$ is 37.6 Hz in aqueous ($^2H_2O$) solution (present work).

were investigated. In addition, a small modification of the standard Dunning contraction scheme, written [5s2p1d|2s], was used since previous work[35] has shown it to yield accurate predictions for $^1J_{CC}$ in ethane and a number of small alicyclic molecules.

For the finite-field perturbation calculations, hypothetical magnetic moments were placed on both coupled nuclei and the coupling constant was determined from the numerical second derivative of the energy shift induced by these moments. As described previously,[35] fields of the order of 0.002 au proved sufficient to maintain numerical accuracy while eliminating higher order contributions to these derivatives.

In order to analyze the effects of various levels of excitations in the correlated QCISD(T) calculations, a complementary set of studies was performed with the related, but simpler, coupled-cluster doubles (CCD) model.[28,29] In this approach the effect of single replacements in the unrestricted Hartree-Fock reference determinant is neglected. An inspection of the corresponding QCISD value then provides a direct estimate of the importance of the relaxation term induced by the presence of amplitudes due to single excitations in the cluster expansion of the SCF wave function. Triple excitations produce further corrections which are recovered only perturbatively in the QCISD(T) model. However, it should be noted that, in the systems studied herein, the triple excitations yield quite negligible contributions to the final value of $^1J_{CC}$.

## Results and Discussion

**A. Basis Set Effects.** The suitability of various standard basis sets currently in common usage for the present correlated calculations of the contact component of indirect nuclear spin–spin coupling has been previously investigated.[35] In a series of calculations on ethane (**12**) in which the experimental coupling is reliably determined and mainly attributed to the Fermi contact mechanism, it was shown that a small modification of the outer-core, inner-valence region of the conventional Dunning double-$\zeta$ contracted Gaussian basis set was sufficient to accurately reproduce the observed coupling. Results from a similar study of the basis set dependence of the contact contribution to $^1J_{CC}$ in ethanol (**10**) are presented in Table I.

At the SCF level, calculations with the valence double-$\zeta$ 6-31G basis set yield a value for $^1J_{CC}$ of 73.1 Hz in **10**, significantly greater than the experimental value (37.6 Hz). Doubling the number of basis functions in the carbon and oxygen cores increases this computed value further, as was observed previously in calculations of $^1J_{CC}$ in **12**.[35] The introduction of polarizing d-functions on carbon and oxygen moderates the SCF value for the coupling constants, but the addition of p-functions on the hydrogens produces little further change. As was observed for **12**, the addition of shells of 6-component d-functions to the split-valence basis set on the heavy atoms reduces the computed SCF coupling constant even more substantially, by more than 11 Hz here. The magnitude of this decrease is attributable to the s-like "extra" component of the Cartesian d-functions in the 6-31G* basis set. This result suggested that a more complete description of the outer-core, inner-valence region of the heavy atoms was necessary. This was achieved as described previously[35] to produce the SCF/[5s2p1d|2s] value of 68.8 Hz for $^1J_{CC}$ (Table I). This modification of the oxygen basis was not required for the SCF calculations but was deemed necessary to prevent imbalances in the heavy-atom descriptions for the correlated calculations.

**Table II.** Correlation Corrections to the Carbon–Carbon One-Bond Nuclear Spin–Spin Coupling Constant, $^1J_{CC}$, in the *Trans* and *Gauche* Conformers of Ethanol[a]

| model (corr) | conformer | |
|---|---|---|
| | *trans* | *gauche* |
| SCF | 68.8 | 65.3 |
| (doubles) | (−33.9) | (−34.0) |
| (singles) | (7.0) | (6.6) |
| (triples) | (−1.1) | (−1.3) |
| QCISD(T) | 40.6 | 36.6 |

[a] Contributions (in hertz) from various levels of excitation within the quadratic configuration interaction model. Calculated for structures described in the text with the [5s2p1d|2s] basis set.

The total correlation corrections to the computed coupling constants are ~20 Hz for the split-valence basis sets and ~30 Hz for the polarized double-$\zeta$ descriptions. This difference conspires to reduce the spread in the computed values at the QCISD(T) level. The second-order perturbation theory estimates of the correlation correction, available from MP2 calculations, range from about 25 Hz for the split-valence bases to greater than 40 Hz for the [4s2p1d|2s1p] basis set. Basis set extension beyond the [5s2p1d|2s] model, through the inclusion of more diffuse and/or more compact s-functions on carbons and a shell of polarizing p-functions on hydrogen, provided little further change in the QCISD(T) values for $^1J_{CC}$. Therefore this description of the single-particle space was adopted throughout the correlated calculations on the glycol conformers.

It should be noted that, even in the gas phase, **10** exists as both *trans* and *gauche* conformers. The results reported in Table I are for the *trans* conformer (defined as having the hydroxyl proton *trans* to $CH_3$) at the geometry cited in Harmony *et al.*[41] attributed to Culot.[42] For the *gauche* conformer, the structure suggested by the microwave study of Sasada *et al.*[43] has been employed to give estimates of $^1J_{CC}$ of 65.3 and 36.6 Hz at the SCF and QCISD(T) levels, respectively, both calculated with the [5s2p1d|2s] basis set. An analysis of the correlation contributions to the [5s2p1d|2s] calculations for the ethanol conformers is presented in Table II.

Corrections due to the presence of amplitudes from double replacements in the SCF wave function are obtained from the CCD model mentioned above. Single excitations are next introduced size-consistently by the QCISD approach. The triples term is recovered perturbatively and is seen to be small. The principal importance of the results presented in Table II is that correlation components remain roughly constant and independent of conformational changes and that the computed differences at the SCF level are nearly the same as in the more complete correlated QCISD(T) calculations.

An estimated energy difference of 0.7 ± 0.1 kcal mol$^{-1}$, with the *trans* conformer being more stable, has been reported between the two ethanol conformers in the gas phase, as deduced from the temperature dependence of vibrational overtones.[44] Differential solvation energetics are likely for the two conformers when in aqueous media, so that a reliable weighting of the computed *ab initio* values is not possible. However, it is expected that the *gauche* conformer will contribute substantially to the observed coupling. Thus the QCISD(T) results, calculated with the [5s2p1d|2s] basis set, for $^1J_{CC}$ in the two conformers should bracket the experimental value, as is observed (Table II).

(41) Harmony, M. D.; Laurie, V. W.; Kuczkowski, R. L.; Schwendeman, R. H.; Ramsay, D. A.; Lovas, F. J.; Lafferty, W. J.; Maki, A. G. *J. Phys. Chem. Ref. Data* **1979**, *8*, 619–721.
(42) Culot, J. P. Ph.D. Thesis, University of Louvain, Belgium, 1971.
(43) Sasada, Y.; Takano, M.; Satoh, T. *J. Mol. Spectrosc.* **1971**, *38*, 33–42.
(44) Fang, H. L.; Swofford, R. L. *Chem. Phys. Lett.* **1984**, *105*, 5–11.

**B. Conformations of Ethylene Glycol (9).** Rotations about three bonds in **9** (C1–O1, C1–C2, C2–O2) generate the full range of available conformations, giving a total of 27 ($3^3$) staggered forms. *Gauche* and *trans* geometries about these bonds are denoted as g (or g′) and t (or t′) for the C–O torsions and G (or G′) and T for the C–C torsion. In this study, the O1–C1–C2–O2 fragment defines the C1–C2 torsion, with $\vartheta_t = 0°$ denoting eclipsed oxygens. C–O torsions are defined by the H–O–C–C fragments, with $\varphi_t = 0°$ denoting eclipsed terminal H and C atoms. Unprimed notation (g, t, G) implies a positive torsion angle produced by a clockwise rotation relative to the initial reference atom, whereas primed notation (g′, t′, G′) implies a negative angle produced by a counterclockwise rotation.

Considerations of molecular symmetry reduce the number of unique conformations of **9** to ten forms. These are: tGt, tGg, tGg′, gGg, gGg′, g′Gg′, tTt, tTg, gTg, and gTg′. Several experimental studies have attempted to elucidate the nature of the conformational preferences exhibited by **9** in a variety of media. For example, only one conformer, tGg′, was detected in a gas-phase microwave study[45] of monodeuterated species. NMR results[46] from nematic–lyotropic solutions apparently also evidence only *gauche* (G) conformers, while a low-temperature infrared study[47] in an argon matrix was interpreted in terms of infrared-induced conformational isomerization (tGg′ → gGg′). The Raman spectrum of an aqueous solution, however, was claimed[48] to show an almost complete absence of intramolecular hydrogen bonding. These reports give access to the earlier experimental literature on **9**.

Many theoretical studies have also been performed on the structures of several conformers of **9**. For example, van Alsenoy *et al.*[49] determined the conformational preferences at the SCF level with a small split-valence 4-21G basis set. These conclusions were recently reinforced by more extensive calculations.[50] In two later works[51,52] the effect of electron correlation on both conformer structure and interconformer energy differences was investigated. Results from HF/6-31G* geometry optimizations on several conformers obtained by Nagy and co-workers,[53,54] including both zero-point energy corrections and an MP2 estimate of the correlation corrections, support the conclusion that tGg′ containing an intramolecular hydrogen bond is the most stable conformer in the gas phase, with gGg′, g′Gg′, and tGt higher in energy by 0.27, 1.02, and 3.02 kcal mol$^{-1}$, respectively. However, subsequent Monte Carlo simulations[53,54] carried out to simulate the effects of aqueous solution on the tGg, gGg′, tGg′, tGt, tTt, and gGg conformers indicate that tGg, which lacks an intramolecular hydrogen bond, is most stable and represents 64% of the conformer population in aqueous solution. The remaining contributing forms are gGg′ (25%), tGg′ (0.08%), and tGt (0.03%). These data support the above experimental evidence that *gauche* forms of **9** predominate in gas and solution ($^2H_2O$) phases. However, some of the quantitative conclusions concerning the differential solvation effects were recently questioned by Hooft *et al.*[55] These references lead to earlier theoretical work on **9**.

(45) Caminati, W.; Corbelli, G. *J. Mol. Spectrosc.* **1981**, *90*, 572–8.
(46) Chidichimo, G.; Imbardelli, D.; Longeri, M.; Saupe, A. *Mol. Phys.* **1988**, *65*, 1143–51.
(47) Takeuchi, H.; Tasumi, M. *Chem. Phys.* **1983**, *77*, 21–34.
(48) Maleknia, S.; Friedman, B. R.; Abedi, N.; Schwartz, M. *Spectrosc. Lett.* **1980**, *13*, 777.
(49) van Alsenoy, C.; van den Enden, L.; Schafer, L. *J. Mol. Struct.* **1984**, *108*, 121.
(50) Vazquez, S.; Mosquera, R. A.; Rios, M. A.; van Alsenoy, C. *J. Mol. Struct.* **1989**, *188*, 95.
(51) Costa Cabral, B. J.; Albuquerque, L. M. P. C.; Silva Fernandes, F. M. S. *Theor. Chim. Acta* **1991**, *78*, 271–80.
(52) Murcko, M. A.; DiPaola, R. A. *J. Am. Chem. Soc.* **1992**, *114*, 10010–8.
(53) Nagy, P. I.; Dunn, W. J., III; Alagona, G.; Ghio, C. *J. Am. Chem. Soc.* **1991**, *113*, 6719–29.
(54) Nagy, P. I.; Dunn, W. J., III; Alagona, G.; Ghio, C. *J. Am. Chem. Soc.* **1992**, *114*, 4752–8.
(55) Hooft, R. W. W.; van Eijck, B. P.; Kroon, J. *J. Chem. Phys.* **1992**, *97*, 3639–46.

**Table III.** Relative Energies of Ethylene Glycol Conformers[a]

| | method | | | |
|---|---|---|---|---|
| conformer | SCF | MP2 | CCD | QCISD(T) |
| tGg′ | 0.0 | 0.0 | 0.0 | 0.0 |
| gGg′ | 0.87 | 0.28 | 0.37 | 0.18 |
| tGt | 3.7 | 4.5 | 4.3 | 4.4 |
| tGg | 4.2 | 4.5 | 4.4 | 4.4 |
| tTt | 2.1 | 3.4 | 3.1 | 3.4 |

[a] Energy differences in kcal mol$^{-1}$ relative to the tGg′ conformer, calculated with the [5s2p1d|2s] basis set at the HF/6-31G*-optimized geometries of the individual conformers.

**Chart I**

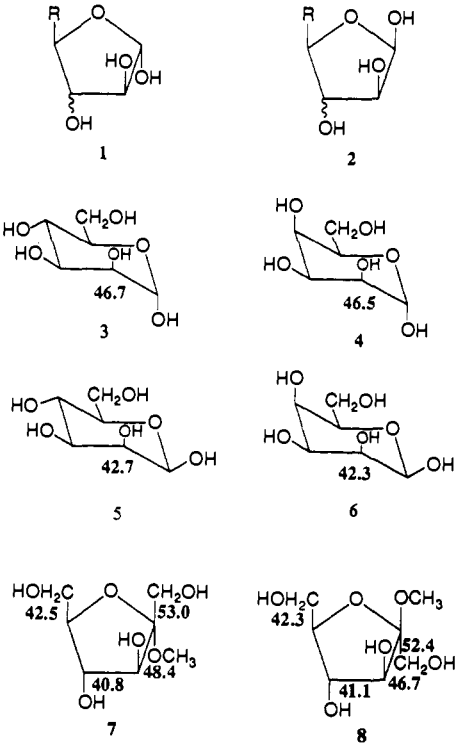


Since the present work includes a much more extensive treatment of the effects of electron correlation in calculations on the conformers of **9**, and since the inclusion of electron correlation appears necessary in determining the relative energies of the conformers, we have collected the results of a series of calculations with the [5s2p1d|2s] basis set in Table III. In agreement with previous studies mentioned above, only a small energy difference (<1 kcal mol$^{-1}$ at the SCF level) separates the two lowest energy conformers, tGg′ and gGg′. The inclusion of electron correlation narrows this energy difference to ~0.3 kcal mol$^{-1}$ at MP2 and still further to <0.2 kcal mol$^{-1}$ at QCISD(T). It should be noted that these calculations are not designed to recover this energy gap accurately, but rather, these results are simply a byproduct of attempts to secure accurate values for $^1J_{CC}$ in the various conformers. However, the results indicate that tGg′ and gGg′ in the gas phase have very similar energies. Correlation effects perturb the energy ordering of the other conformers. In particular, the relative energies of both tGt and tTt are substantially increased at the QCISD(T) level, although this increase is now slightly moderated from the corresponding MP2 results.

**C. Effect of Electronegative Substituents on $^1J_{CC}$.** An inspection of $^1J_{CC}$ values in **7** and **8** (Chart I) shows that their magnitudes depend on the number of oxygen substituents appended to the coupled carbons.[56] $^1J_{CC}$ increases with the number of oxygen substituents on the C–C fragment. Thus, $^1J_{C1,C2}$ (52.7 ± 0.3 Hz) is ~10 Hz larger than $^1J_{C5,C6}$ (42.4 ± 0.1 Hz) in **7** and **8**; the

(56) Duker, J.; Serianni, A. S. *Carbohydr. Res.*, in press.

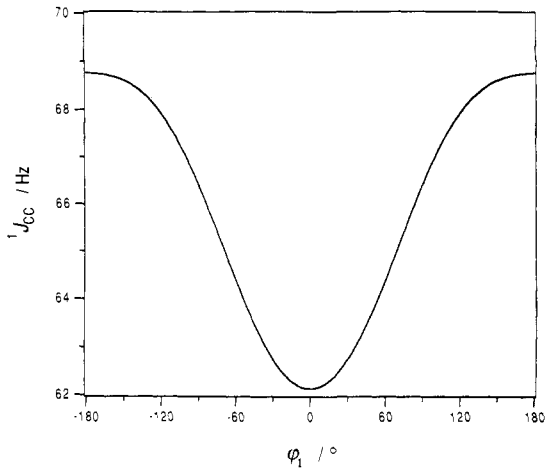


**Figure 1.** Variation of the one-bond spin–spin coupling constant, $^1J_{CC}$ (Hz), in **10** as a function of torsion, $\varphi_t$, about the C–O bond. $\varphi_t = 180°$ in the *trans* conformation. Calculations are at the Hartree–Fock level with the [5s2p1d|2s] basis set. Correlation corrections shift this curve downward by ~28.4 Hz.

**Table IV.** Substituent and Conformational Effects on Calculated[a] and Experimental Values of $^1J_{CC}$

| molecule | method | | |
|---|---|---|---|
| | SCF | QCISD(T) | expt |
| ethane (**12**) | | | 34.6[b] |
| staggered | 61.6 | 34.1 | |
| ethanol (**10**) | | | 37.6[c] |
| *trans* | 68.8 | 40.7 | |
| *gauche* | 65.3 | 36.6 | |
| ethylene glycol (**9**) | | | |
| tGg′ | 70.1 | 40.5 | |
| gGg′ | 67.9 | 37.7 | |
| tGt | 75.6 | 46.2 | |
| tGg | 71.6 | 41.5 | |
| tTt | 77.6 | 48.7 | |
| 1,2-dihydroxypropane (**13**) | | | 41.3[d] |
| glycolaldehyde hydrate (**11**) | | | 48.7[e] |

[a] Fermi contact component calculated with the [5s2p1d|2s] basis set at experimental geometries for **10** and **12**; others are for HF/6-31G*-optimized structures. Values reported in hertz. [b] Reference 57. [c] In $^2H_2O$ (present work). [d] $^1J_{C1,C2}$ (present work). [e] Reference 39.

former pathway contains three oxygen substituents (O1, O2, O5) while the latter contains two (O5, O6). Likewise, $^1J_{C2,C3}$ (47.1 ± 1.2 Hz) is ~7 Hz larger than $^1J_{C3,C4}$ (40.4 ± 0.9 Hz), since the former C–C bond contains an additional oxygen substituent.

Values of $^1J_{CC}$ in ethane (**12**) (34.6 Hz),[57] ethanol (**10**) (37.6 Hz in $^2H_2O$), [1-$^{13}$C]-1,2-dihydroxypropane (**13**) (41.3 Hz in $^2H_2O$), and glycolaldehyde hydrate (**11**) (48.7 Hz in $^2H_2O$)[39] confirm the substituent dependency of $^1J_{CC}$ observed in **7** and **8** (Table IV). Computed $^1J_{CC}$ values in **9**–**12** determined at the SCF and QCISD(T) levels follow the same trends observed in the experimental values, thus validating the computational approach (Table IV). $^1J_{CC}$ values determined by QCISD(T), of course, are in much closer agreement with experimental data than SCF-derived couplings (Table IV). More importantly, calculated values of $^1J_{CC}$ in **9** and **10** depend on conformation. For example, $^1J_{CC}$ responds to the C–O torsion angle in **10** and is larger when C2 and OH1 are *trans* as opposed to *gauche*. This is clearly demonstrated in Figure 1, where the variation in $^1J_{CC}$ computed at the SCF/[5s2p1d|2s] level with torsion around the C–O bond is displayed. This curve is derived from the results of a series of calculations performed at points reached by rigid rotations in 15° increments about the C–O bond starting from the *trans* conformation ($\varphi_t = 180°$). As indicated in Table II, correlation corrections to these SCF values are roughly independent of torsion angle so that the QCISD(T) values for the coupling constant are expected to mimic this functional behavior. This expectation is confirmed by comparing the SCF and QCISD(T) results obtained for the extremal values of $^1J_{CC}$ on this curve. At $\varphi_t = 180°$ the SCF value of 68.8 Hz is reduced to 40.7 Hz at the QCISD(T) level, a reduction of 28.1 Hz, while at $\varphi_t = 0°$ the corresponding decrement upon the inclusion of electron correlation is 28.3 Hz in the SCF value of 61.1 Hz.

**Table V.** Correlation Corrections to $^1J_{CC}$ in Conformers of Ethylene Glycol[a]

| model (corr) | conformer | | |
|---|---|---|---|
| | tGg | gGg′ | tTt |
| SCF | 71.6 | 67.9 | 77.6 |
| (doubles) | (−35.7) | (−35.4) | (−34.8) |
| (singles) | (6.9) | (6.6) | (7.1) |
| (triples) | (−1.4) | (−1.5) | (−1.2) |
| QCISD(T) | 41.5 | 37.6 | 48.7 |

[a] Contributions (in hertz) from various levels of excitation within the quadratic configuration interaction model. Calculated for HF/6-31G*-optimized structures with the [5s2p1d|2s] basis set.

$^1J_{CC}$ in the four preferred *gauche* geometries of **9** in aqueous solution differ by 8.5 Hz; the minimal value (37.7 Hz) is obtained when O1–H and O2–H are *gauche* to C2 and C1, respectively (gGg′), while the maximal value (46.2 Hz) is obtained when O1–H and O2–H are *trans* to C2 and C1, respectively (tGt). On the basis of the solution proportions of these four *gauche* forms calculated by Nagy and co-workers[53,54] (see above), a weighted-average $^1J_{CC}$ of 40.4 ± 0.6 Hz is predicted for **9** in aqueous solution. This result is in close accord with the value deduced by comparison of the known splittings in **10** (37.3 Hz) and 2-propanol (**14**) (38.6 Hz), where methyl substitution on the hydroxyl-bearing carbon is seen to lead to a small increase in $^1J_{CC}$,[58] with that measured for **13** (41.3 Hz) in this work.

An analysis, similar to that given in Table II for **10**, of the correlation corrections to the SCF value of $^1J_{CC}$ for several conformers of **9** is presented in Table V. Despite the wide range in computed coupling constants for the chosen conformers, correlation effects are seen to be roughly independent of conformation. Calculations on other conformers display the same behavior. The doubles contribution is ~1 Hz more negative than that computed in **10**, while the other components are basically unchanged. The total correlation corrections to the SCF coupling constants in the various conformers of **9** are thus only slightly greater (~1 Hz) than those recovered in calculations on the singly hydroxylated molecule. Averaging over the values obtained for the four conformers discussed here provides a reduction factor of 29.8 ± 0.4 Hz for **9** with this particular [5s2p1d|2s] basis set. This result is comparable to the corresponding factors of 28.4 ± 0.3 Hz derived for **10** above and 27.5 ± 0.2 Hz for **12** reported previously.[35]

**D. Effect of C–C and C–O Torsions on $^1J_{CC}$ in 9.** A conformational energy profile for **9** (Figure 2) was generated in which the C1–C2 bond in the starting conformation, tGt ($\vartheta_t$ = 72.6°), was rotated $2\pi$ radians in 15° increments without allowing any relaxation in the other geometrical parameters. As expected, minima are observed at $\vartheta_t$ = ~60° (tGt), ~180° (tTt), and ~300° (tG′t); the maximal energy form at $\vartheta_t$ = ~360° has both oxygen atoms eclipsed or nearly eclipsed. While this torsional potential energy curve was obtained at the SCF level (with the [5s2p1d|2s] basis set), the inclusion of electron correlation does not significantly alter the location of these features.

The dependence of $^1J_{CC}$ on C1–C2 and C1–O1 bond rotations, again using tGt as an initial geometry, is illustrated in Figure 3. This hypersurface is obtained from the results of a series of SCF/[4s2p1d|2s1p] calculations performed at points spaced equidis-

(57) Lynden-Bell, R. M.; Sheppard, N. *Proc. R. Soc.* **1962**, *269A*, 385.

(58) Summerhays, K. D.; Maciel, G. E. *J. Am. Chem. Soc.* **1972**, *94*, 8348–51.

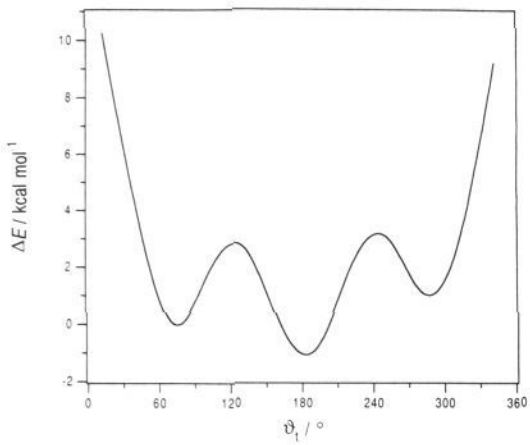


**Figure 2.** Variation in the HF/[5s2p1d|2s] energy, $\Delta E$ (kcal mol$^{-1}$), in **9** (tGt conformer) with torsion about the C–C bond. $\vartheta_t = 72.6°$ for the tGt conformer.

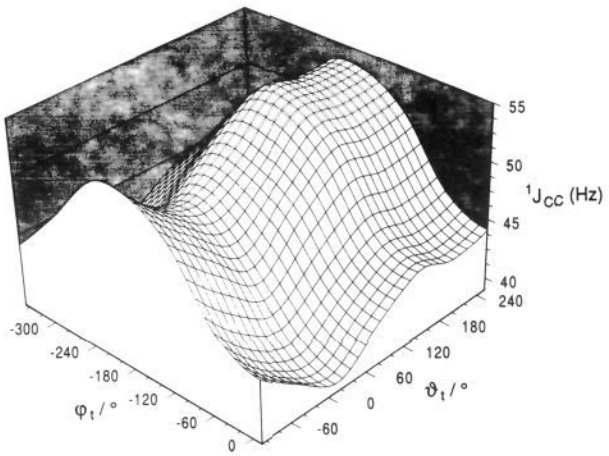


**Figure 3.** Variation of $^1J_{CC}$ in **9** with torsions about the C–O and C–C bonds. The surface was generated by rigid ($\vartheta_t$, $\varphi_t$) rotations from the tGt conformer ($\vartheta_t = 72.6°$, $\varphi_t = -166.2°$). Shifted results are from HF/[4s2p1d|2s1p] calculations. See text.

tantly from the tGt origin ($\vartheta_t = 72.6°$; $\varphi_t = -166.2°$). The results of the SCF calculations are then shifted downward by a constant amount as described above to reflect the expected correlated values. It may be seen that, for C–C torsions with a given C–O dihedral angle, $^1J_{CC}$ is minimal when O1 and O2 are eclipsed or nearly eclipsed, whereas maximal values are observed when these oxygens are widely separated ($\vartheta_t \sim 180°$). This result is consistent with the observed dependence of $^1J_{CC}$ in carbohydrates.[15,24-27] Furthermore, for C–O torsions with a given C–C dihedral angle, $^1J_{CC}$ in **9** is minimal when OH1 and C2 are eclipsed and maximal when these atoms are *trans*, in agreement with observations made on **10** (see above).

A related hypersurface (Figure 4) generated by a similar set of SCF/[4s2p1d|2s1p] calculations from an initial gGg′ geometry ($\vartheta_t = 59.7°$; $\varphi_t = 76.0°$, $\varphi_{t'} = -46.7°$) reveals similar trends. The surface is obtained by stepping in 30° increments along $\vartheta_t$ and $\varphi_{t'}$ only; the conformation around the g-center remains unchanged. 1D slices at 0° on both axes of Figure 4 (Figure 5A,B) show a variation in $^1J_{CC}$ of ~8 Hz due to C–O rotation, whereas C–C bond rotation causes a smaller fluctuation (~5 Hz) in $^1J_{CC}$. The data points for Figure 5 have been recomputed using the slightly different [5s2p1d|2s] basis set to better allow comparison with the results of correlated calculations on the various conformers listed in Table IV. Once again note that the curves displayed in Figure 5 are obtained from SCF calculations which are then shifted downward by a constant amount (29.8 Hz) to account for

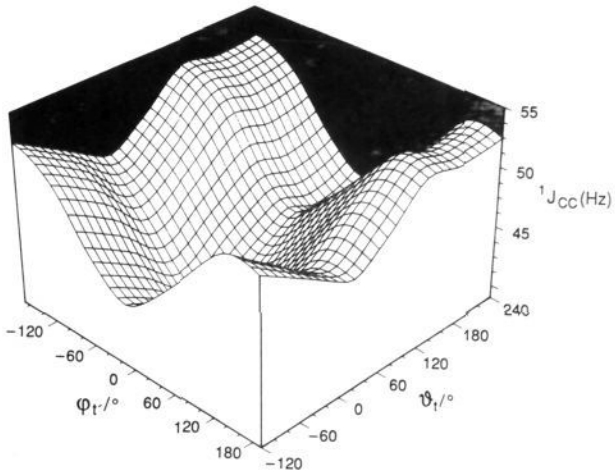


**Figure 4.** Variation of $^1J_{CC}$ in **9** with torsions about the C–O(g′) and C–C bonds. The surface was generated by rigid ($\vartheta_t$, $\varphi_{t'}$) rotations from the gGg′ conformer ($\vartheta_t = 59.7°$, $\varphi_t = 76.0°$, $\varphi_{t'} = -46.7°$). Shifted results are from HF/[4s2p1d|2s1p] calculations. See text.

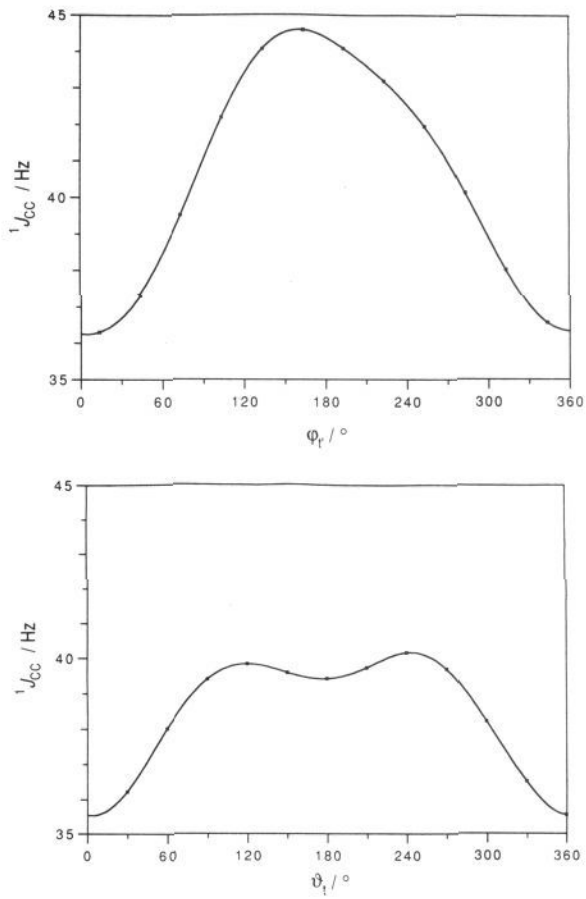


**Figure 5.** Variation of $^1J_{CC}$ in **9** (gGg′ conformer) as a function of (A, top) torsion, $\varphi_t$, about the C–O(g′) bond ($\varphi_{t'} = -46.7°$ (≡313.3°)) and (B, bottom) torsion, $\vartheta_t$, about the C–C bond ($\vartheta_t = 59.7°$) in the gGg′ conformation. Shifted results are from HF/[5s2p1d|2s] calculations. See text.

the inclusion of electron correlation. Several single-point calculations have been performed at geometries which provide nearly extremal values on these curves, and in agreement with the conclusions reached above for single-point calculations on specific conformers of **9**, correlation corrections are roughly constant.

It should also be noted that, in the course of these torsional excursions from the original conformation, the molecular structure passes "close" to the geometry of some other fully relaxed

**Chart II**

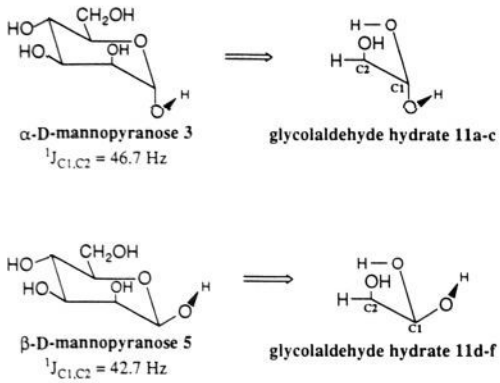


conformers. For example, starting from gGg′, the CO(g′) torsion leads to tGg (when $\varphi_{t'} \sim 180°$) and gGg (when $\varphi_{t'} \sim 45°$) and the CC torsion approaches gTg′ ($\vartheta_t \sim 180°$). QCISD(T)/[5s2p1d|2s]2] calculations of $^1J_{CC}$ for the fully optimized tGg, gGg, and gTg′ conformers indicate that the combined effect of all other structural relaxations produces changes from the rigid-rotation values of less than 3 Hz in the computed coupling constants.

The finding that the magnitude of the changes in $^1J_{CC}$ induced by torsions about the C–O bond is greater than that caused by C–C rotation is of particular importance when coupling data are employed to assign configuration and/or conformation in carbohydrates. A simplistic explanation of the observed differences in $^1J_{CC}$ has previously been sought in O–C–C–O dihedral angles. These data now show that the orientation of the C–O bonds must also be considered in the analysis.

**E. Effect of C–C and C–O Torsions on $^1J_{CC}$ in 11: A Mannopyranose Model.** Computed $^1J_{CC}$ values for a range of conformers of **9** (Table IV; Figures 3–5) provide a theoretical basis for empirically derived correlations made in **1–8** (Chart I) between $^1J_{CC}$ and the relative orientation of hydroxyl groups on CC fragments. However, the use of **9** as a model compound to explain torsion effects on $^1J_{CC}$ in carbohydrates is limited, in principle, to HO–C–C–OH fragments only (e.g., $^1J_{C3,C4}$ in **7** and **8**). $^1J_{CC}$ behavior in $(OH)_2$–C–C–OH fragments, such as the C1–C2 fragment found in aldofuranosyl (**1, 2**) and aldopyranosyl rings (**3–6**), may not be reliably predicted from studies of **9**. The fact that both C–C and C–O torsions affect the magnitude of $^1J_{CC}$ in **9** (and presumably $(OH)_2$–C–C–OH fragments), and that it might be desirable to identify a system in which both C–C *and* C–O torsions may be assessed experimentally, provides an impetus to examine $^1J_{CC}$ in $(OH)_2$–C–C–OH fragments. For example, in α-D-mannopyranose (**3**) and β-D-mannopyranose (**5**), the C1–C2 torsion angles are fixed (~180 and ~60°, respectively). In addition, however, the C1–O1 torsions in **3** and **5** are also expected to have preferred conformations induced by stereoelectronic effects at the anomeric center; the exoanomeric effect[59,60] in **3** and **5** should stabilize those torsions in which the anomeric hydroxyl proton is *gauche* to H1 and O5. Thus, **3** and **5** are attractive model systems since two of the three torsions that affect $^1J_{C1,C2}$ are either fixed or restricted. Since $^1J_{C1,C2}$ have been measured in **3** and **5** (Chart I), it remains to obtain experimental evidence for the preferred C1–O1 and C2–O2 torsions in these molecules and to compute $^1J_{CC}$ in appropriate model fragments for comparative purposes.

The C1–C2 fragments in **3** and **5** may be modeled by glycolaldehyde hydrate (**11**), as illustrated in Chart II. Substitution of OH1′ for C5, and H2 for C2, is not expected to have

(59) Lemieux, R. U. *Pure Appl. Chem.* **1971**, *25*, 527–48.
(60) Lemieux, R. U.; Koto, S.; Voisin, D. In *Anomeric Effect: Origin and Consequences*; Szarek, W. A., Horton, D., Eds.; ACS Symposium Series 87; American Chemical Society: Washington, DC, 1979; p 17.

**Chart III**

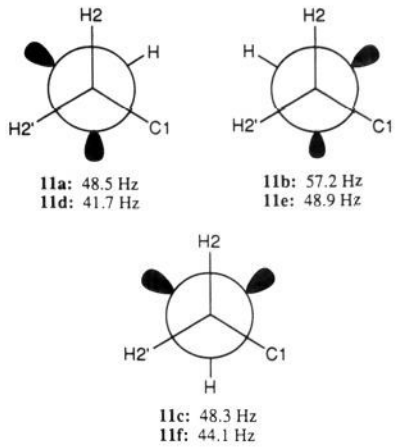


a large effect on the magnitude of $^1J_{CC}$. Furthermore, to restrict the number of C–O conformations to be studied, the C1–O1 torsion was chosen to optimize the exoanomeric effect as discussed above; in contrast, all three staggered C2–O2 rotamers were examined. All other geometrical parameters were allowed to relax by optimizing the remaining degrees of freedom in an SCF/6-31G* calculation. Thus, $^1J_{CC}$ values were computed at the SCF level using the [5s2p1d|2s] basis set for glycolaldehyde hydrate conformations that correspond, in terms of C–C torsion, to those found in **3** (**11a–c**) and **5** (**11d–f**). $^1J_{CC}$ were subsequently shifted downward by a factor of 31.6 Hz to yield couplings expected from QCISD(T) methods on the basis of results derived from the complete QCISD(T) calculations on the conformers of **12**, **10**, and **9**. As shown in Chart III, the computed $^1J_{CC}$ for **11a–c** range from 48.3 to 57.2 Hz, depending on the C2–O2 torsion; by comparison, $^1J_{C1,C2}$ = 46.7 Hz in **3**.[15] As expected, the computed $^1J_{CC}$ is larger in **11b** (57.2 Hz) than in **11a** and **11c** (48.5 and 48.3 Hz, respectively), as OH2 is anti to C1 in the former. In contrast, computed $^1J_{CC}$ in **11d–f** range from 41.7 to 48.9 Hz; by comparison, $^1J_{C1,C2}$ = 42.7 Hz in **5**.[15] Again, the largest coupling is observed in **11e** in which OH2 is anti to C1. Thus, the effect of C–C and C–O torsions on $^1J_{CC}$ in glycolaldehyde hydrate models appears similar to that observed in **9**, and the computed $^1J_{CC}$ in **11a–c** and **11d–f** correspond closely to $^1J_{C1,C2}$ in **3** and **5**, respectively. The validity of the correction factor was further checked by comparing the modified SCF/[5s2p1d|2s] predictions for **11a** and **11d** with the results of QCISD/[5s2p1d|2s] calculations for the same structures. In each case the shifted SCF value was less than 0.4 Hz below the actual QCISD result, after adjusting the shifting factor to take into account the lack of a contribution from triples amplitudes in the QCISD calculation, the inclusion of which would have been computationally too expensive.

A more careful evaluation of the degree of agreement between computed $^1J_{CC}$ in glycolaldehyde hydrate models **11a–f** and experimental $^1J_{C1,C2}$ in **3** and **5** requires information on the C1–O1 and C2–O2 torsions in **3** and **5**. These torsions have been inspected in **3** by measuring $^3J_{HCOH}$ and $^3J_{CCOH}$ involving the hydroxyl protons at C1 and C2 in a DMSO-$d_6$ solvent; such a determination could be made for **3** since this anomer of D-mannopyranose is readily obtained in crystalline form. A Karplus equation relating the C–O dihedral angle to $^3J_{HCOH}$ has been proposed,[6] whereas $^3J_{CCOH}$ may be used only qualitatively at present.[61] The latter couplings were measured in [1-$^{13}$C]**3** and [2-$^{13}$C]**3** in DMSO-$d_6$, and the observation of these couplings also served to confirm the hydroxyl proton resonance assignments for **3**. For **3** in DMSO-$d_6$, $^3J_{H1,C1,O1,H}$ = 4.3 Hz and $^3J_{C2,C1,O1,H}$ = 6.9 Hz. These data are consistent with a preferred C1–O1 torsion angle having OH1 *gauche* to H1 and O5 (i.e., OH1 and

(61) Dais, P.; Perlin, A. S. *Can. J. Chem.* **1982**, *60*, 1648.

C2 *trans*), as expected from the exoanomeric effect. $^3J_{H2,C2,O2,H}$ = 4.3 Hz and $^3J_{C1,C2,O2,H}$ = 4.4 Hz in **3**, data which are consistent with preferred C2–O2 torsions having OH2 *gauche*, rather than *trans*, to H2. On the basis of the moderately small value for $^3J_{C1,C2,O2,H}$ (compared to $^3J_{C2,C1,O1,H}$), it appears that, of the two conformers having OH2 *gauche* to H2, that having OH2 *gauche* to C1 is more favored than that having OH2 *gauche* to C3. If these interpretations are correct, and if it is assumed that C–O torsional behaviors in **3** are similar in DMSO-$d_6$ and $^2H_2O$, then **11a** may be considered the preferred model of **3**, and the computed value of 48.5 Hz for **11a** agrees well with the value of $^1J_{C1,C2}$ (46.7 Hz) found in **3**.

## Conclusions

The key findings of this study may be summarized as follows: (a) $^1J_{CC}$ values increase as the number of hydroxyl substituents on the CC fragment increases. (b) $^1J_{CC}$ values may be computed with considerable accuracy using QCISD(T) methods. Electron correlation contributions are insensitive to conformation, so that *changes* in $^1J_{CC}$ with conformation may be determined from much simpler SCF methods. (c) Good agreement is found between the observed behavior of $^1J_{CC}$ in carbohydrate structures and the calculated values of $^1J_{CC}$ in model compounds. (d) As predicted from observations made in a variety of carbohydrate systems, $^1J_{CC}$ depends on the C–C torsion angle in HO–C–C–OH fragments. Coupling is nearly maximal when the hydroxyl substituents are *trans* and falls to a minimum as the eclipsed geometry is approached. (e) In addition to C–C torsion, $^1J_{CC}$ in ethylene glycol fragments also depends on the C–O torsions; geometries in which the hydroxyl proton is anti to a carbon give the maximum or nearly maximum coupling. The variation in $^1J_{CC}$ with torsion about C–O bonds is more pronounced than that induced by torsions about the C–C bond. (f) Correlations made between C–C and C–O torsions and $^1J_{CC}$ in ethylene glycol fragments appear to be maintained in glycolaldehyde hydrate fragments.

The impetus for this study was embodied in the expectation that $^1J_{CC}$ values in carbohydrates and carbohydrate-containing compounds might be useful in establishing configuration and conformation. The experimental and computational results show the magnitude of $^1J_{CC}$ to depend on C–C torsion as expected, but the C–O torsions are also critical determinants. This latter factor would appear to impose limitations on the use of $^1J_{CC}$ as a structural probe. However, in cases where one of these variables can be defined via other experimental parameters, $^1J_{CC}$ may provide useful structural information. For example, if the C–C torsion can be defined independently, then $^1J_{CC}$ may be used to assess hydroxyl proton orientation (i.e., C–O torsion) in aqueous solution, information which is not readily available at present. The results of this study provide an improved understanding of the effects of molecular geometry on $^1J_{CC}$ in HO–C–C–OH and related fragments that must be considered in future efforts to develop $^1J_{CC}$ as a potential structural probe.

**Acknowledgment.** The research described herein has been supported by the Office of Basic Energy Sciences of the U.S. Department of Energy and by Omicron Biochemicals, Inc., of South Bend, IN.